COVRA Salt Creep Modelling – PA model

Modelling Report

Quintessa Document Owner: Josh Nicholas and Kate Thatcher
Client: COVRA
Document Id: QDS-10133A-R1
Version: 2
Date: 18/07/2023

1 Introduction

An advantage of using salt host rocks for geological disposal of radioactive waste is that the galleries and boreholes constructed within the salt can be backfilled with the excavated material, and that both the in-situ salt and the crushed rock backfill are expected to creep on relatively short timescale, to create low porosity and low permeability barriers to radionuclide migration.

van Oosterhout et al. (2022a) reviewed the processes leading to creep in crushed salt rock backfill and proposed a numerical model to account for both the convergence of the gallery and the compaction of the backfill. The current project takes this numerical model and implements it in COMSOL Multiphysics®. For the present work, only the convergence in the backfill is represented explicitly in the model.

In the current report, we describe the model (Section 2) and the implementation in COMSOL Multiphysics® (Section 3). We then report testing of the model both as a stand-alone model (Section 4) and coupled to Richards' Equation (Section 5). Some conclusions and ideas for further work are presented in Section 6.

2 Model

van Oosterhout et al. (2022a) present a model for the rate of change of porosity ($\dot{\phi}$) as a function of mean Terzaghi effective stress ($\bar{\sigma}$) and porosity (ϕ) in Equation 5.18:

$$\dot{\phi} = -(100 - \phi)(B_1 \bar{\sigma}^{m_1} f_1(\phi) + B_2 \bar{\sigma}^{m_2} f_2(\phi)) \quad \text{Eq. 1}$$

The two parts of the equation represent dislocation creep (subscript 1) and humidity-assisted diffusion creep (subscript 2). Parameters B, m and f are defined in Table 4-1 (van Oosterhout et al., 2022a), presented here in Table 1. This equation is expected to be valid in the porosity range 40% – 1%. The grainsize of the backfill is expected to be in the

range 0.1 to 10 mm with 85% of grains in the range 0.1-0.5 mm and 15% of grains in the range 2-10 mm.

Table 1: Parameterisation of Equation 1, taken from van Oosterhout et al. (2022a), Table 4-1. R is the ideal gas constant (8.314 J mol^{-1} K^{-1}), T is temperature and d_b is the grainsize of the backfill.

Dislocation creep	Diffusion / humidity creep
$B_1 = A_N \exp\left(\frac{-Q_N}{RT}\right)$	$B_2 = A_{hum} \exp\left(\frac{-Q_{ps}}{RT}\right) 1/T{d_b}^3$
$m_1 = 5$	$m_2 = 1$
$f_1(\phi) = \left(\frac{0.01648}{\left(0.0003 - \frac{1}{\phi_0^{0.1}} + \frac{1}{\phi^{0.1}}\right)^{2.25}} \right)^{\frac{3}{5}}$	$f_2(\phi) = 9.74 \times 10^{-4} \phi^{2.589}$
$A_N = 1.09 \times 10^{-6}$ MPa^{-5} s^{-1}	$A_{hum} = 3.8 \times 10^{-14}$ MPa^{-1} s^{-1} K m^3
$Q_N = 54$ kJ mol^{-1}	$Q_{ps} = 24.53$ kJ mol^{-1}

To solve Equation 1, a relationship between porosity and stress is needed. Equation 5.17 of van Oosterhout et al. (2022a) (Equation 2) is derived from balancing the strain rate in the in-situ salt around the gallery with the strain rate in the backfill. This assumes that no pore pressure builds up during convergence.

$$\alpha_1 A_1 (P - \bar{\sigma})^{n_1} + \alpha_2 A_2 (P - \bar{\sigma})^{n_2} - \left(B_1 \bar{\sigma}^{m_1} f_1(\phi) + B_2 \bar{\sigma}^{m_2} f_2(\phi)\right) = 0 \qquad \text{Eq. 2}$$

The first two terms of Equation 2 represent strain rate in the in-situ salt rock and the third and fourth terms represent strain rate in the backfill. P is lithostatic pressure and $\alpha_i = \left(3^{\frac{n_i+1}{2}}\right)/n_i^{n_i}$. Parameters for the in-situ salt rock are given in Table 2.

Table 2: Additional parameterisation for Equation 2, taken from van Oosterhout et al. (2022), Table 4-1. Typical grainsize for the in-situ salt rock is suggested to be d_h = 5 mm, with a range of 2-10 mm valid.

Dislocation creep	Pressure solution creep
$A_1 = A_{dc} \exp\left(\frac{-Q_{dc}}{RT}\right)$	$A_2 = A_{ps} \exp\left(\frac{-Q_{ps}}{RT}\right) 1/T{d_h}^3$
$n_1 = 5$	$n_2 = 1$
$A_{dc} = 2.1 \times 10^{-6}$ MPa^{-5} s^{-1}	$A_{ps} = 3.8 \times 10^{-13}$ MPa^{-1} s^{-1} K m^3
$Q_{dc} = 54$ kJ mol^{-1}	$Q_{ps} = 24.53$ kJ mol^{-1}

3 Implementation in COMSOL

The model described in section 2 has been implemented in the COMSOL Multiphysics® files, 'CreepModel_simplifiedGeometry.mph' and CreepModel_fullGeometry.mph', delivered alongside this report. The following section steps through and explains the key components of the COMSOL implementation. Note that text formatted as `code` refers to variable names in the model.

Firstly, several parameters are defined in the global domain. These are the initial and final porosities, which are given as percentages and defined as $\phi_0 = 40$ (`Crushed_Salt_Initial_Porosity`) and $\phi_f = 0.1$ (`Crushed_Salt_Final_Porosity`) respectively. The starting porosity used by the solver, `Starting_Porosity`, is set to match the initial porosity, although could be changed. The rest of model is implemented under a single component node, which should contain the geometry of the system being modelled, and any other processes which occur alongside the salt creep.

The model includes two dependent variables and their associated ODEs, porosity, represented by `por`, and mean Terzaghi effective stress, represented by `s` (stress is not formally a dependent variable in a mathematical sense, but was defined in this way for convenience). The model contains two domain ODE nodes, and each node then contains a distributed ODE of the form

$$e_a \frac{\partial^2 u}{\partial^2 t} + d_a \frac{\partial u}{\partial t} = f \qquad \text{Eq. 3}$$

where u is the dependent variable, e_a and d_a are coefficients, and f is the source term. These ODEs apply to all model domains where the crushed salt is present. Table 3 shows the coefficients, source terms and initial conditions used for the two ODEs.

The purpose of the "Porosity Model" ODE is to solve Eq. 1 to calculate porosity as a function of time. Variables related to this ODE are defined under the node "Salt Creep Porosity". `Porosity_Rate_Salt` is set to the expression for $\dot{\phi}$ in Eq. 1. Similarly, ϕ is represented by the variable `Porosity_Salt`, which is set equal to the dependent variable `por`. However, porosity is not allowed to decrease below its final value. To achieve this, once `por` falls below ϕ_f, `Porosity_Rate_Salt` is set to zero and `Porosity_Salt` is set to ϕ_f. (For this reason, `Porosity_Salt` should be coupled to other processes in the model rather than `por`.)

The purpose of the "Stress with Porosity" ODE is to calculate stress for a given porosity by solving the algebraic equation in Eq. 2. The terms `Strain_Rate_1` to `Strain_Rate_4` correspond to the four strain terms in this equation, and are defined under the node "Salt Creep Strain Rates". Note that the initial value for stress is not the actual stress at t=0, but an initial guess used by the solver. This variable, `Initial_S`,

should be set to a reasonable value to allow COMSOL to solve Eq. 2. By trial and error, 0.5 MPa was found to be an appropriate value for the current cases.

The remaining parameters described in section 2 have then been implemented as variables under the node "Salt Creep Definitions". The names of these variables correspond to the symbols used in this report. Note that temperature is assumed to be homogenous throughout the model domain.

Table 3: Domain ODEs used in the COMSOL implementation, and their coefficients, source terms, and initial values.

	Porosity Model	**Stress with Porosity**
u	`por`	`s`
e_a	0	0
d_a	1	0
f	`Porosity_Rate_Salt`	`Strain_Rate_1 + Strain_Rate_2 - (Strain_Rate_3 + Strain_Rate_4)`
$u(t=0)$	`Starting_Porosity`	`Initial_S`
$\dot{u}(\mathrm{t}=0)$	0	0

For the purposes of testing the creep model on its own (see section 0), a placeholder geometry of a 1D line interval spanning coordinates 0 to 1 was defined. The geometry used to test the model when coupled to Richards' Equation is described in section 5.

4 Static Testing

To test the implementation of the model in COMSOL, three model studies are presented:

A. Reproduction of results from van Oosterhout et al. (2022b) for convergence with only humidity creep in the backfill, for three fixed grainsizes in the backfill;
B. An extension of Case A to include both humidity and dislocation creep in the backfill, for three fixed grainsizes in the backfill;
C. An extension of Case B to include an illustrative temperature change, representative of heating due to radioactive waste disposal.

All three cases are calculated for three grainsizes in the backfill, $d_b = 0.3$ mm, $d_b = 1.0$ mm and $d_b = 3.0$ mm, and assuming a grainsize in the in-situ salt rock of $d_h = 5$ mm. In Case A and B, temperature is assumed to be 39.85°C. Lithostatic pressure is assumed to be P = 15 MPa. All other parameters are as given in Section 2.

Since there are only independent results for Case A, the model has also been implemented in Quintessa's code QPAC to check for errors in the implementation.

4.1 Case A

Results from both the COMSOL and QPAC implementations of the creep model agree very well with results from van Oosterhout et al. (2022b), providing confidence in the implementation of the model in COMSOL (Figure 4-1 and Figure 4-2).

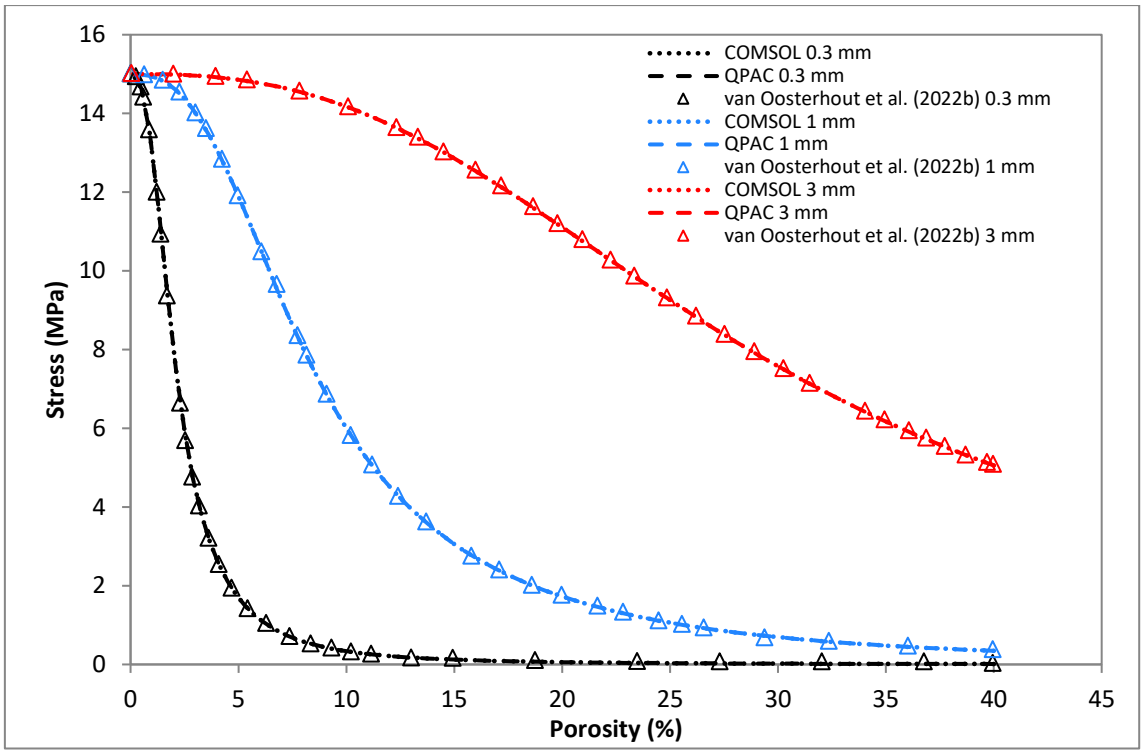

Figure 4-1: Mean Terzaghi effective stress against porosity for three backfill grain sizes (Case A)

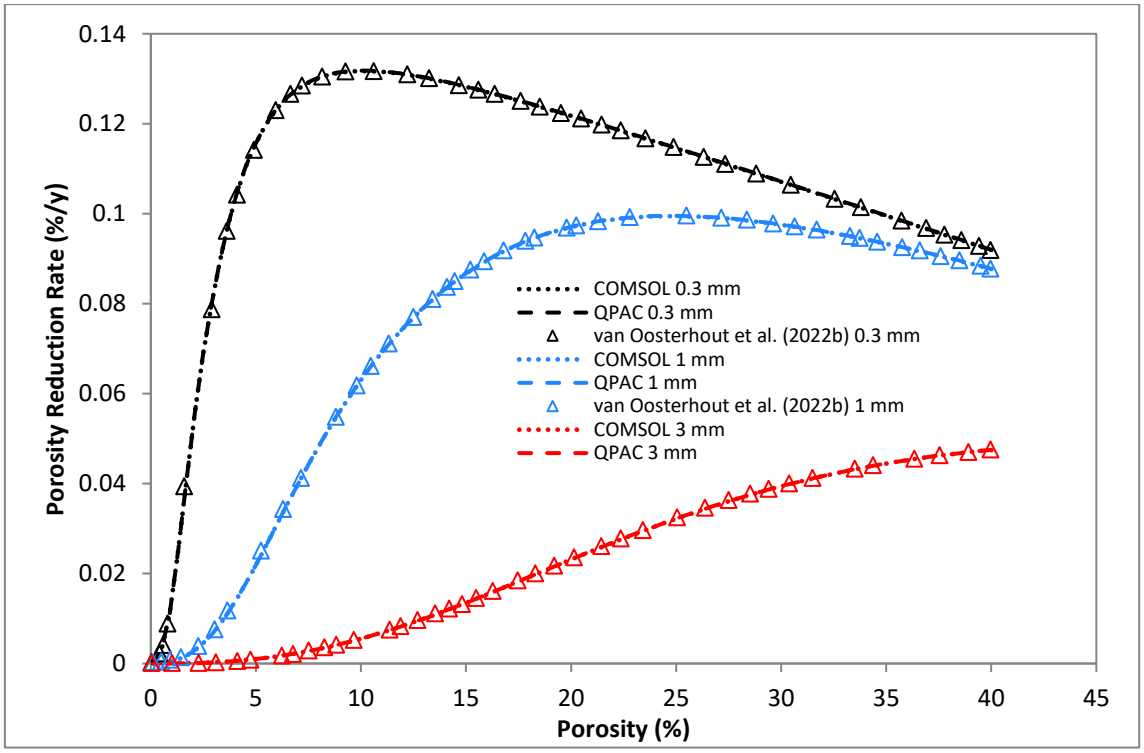

Figure 4-2: Porosity reduction rate against porosity for three backfill grain sizes (Case A)

4.2 Case B

Good agreement was obtained between the COMSOL and QPAC results for Case B (Figure 4-3 and Figure 4-4), providing confidence in the implementation. Although there are no independent results to compare against in this case, the impact of the additional dislocation creep term on the results can be determined qualitatively from study of Eq. 1.

From study of the relative magnitude of terms in Eq. 1, it can be seen that for low stresses, humidity creep will dominate, whereas for high stresses, dislocation creep will dominate (since stress is raised to the power 5 for dislocation creep). In addition, humidity creep is proportional to $1/{d_b}^3$ so gets smaller rapidly as grainsize increases, whereas dislocation creep is independent of grainsize. This means that for small grainsizes, we would expect humidity creep to dominate dislocation creep at lower stresses (high porosity) and dislocation creep to become increasingly significant at higher stresses (low porosity). For bigger grainsizes, humidity creep with be small compared with dislocation creep at all grainsizes.

Comparing the Case B results with the reference Case A results (Figure 4-3 and Figure 4-4), for $d_b = 0.3$ mm and $d_b = 1.0$ mm, shows the two cases are equivalent for higher porosities but deviate at lower porosities. This is consistent with the above analysis. At lower porosities, the addition of the dislocation creep term increases the strain rate in the backfill. This means that the resistance provided by the backfill against the in-situ salt decreases faster for Case B than Case A, and consequently the stress in the backfill increases more slowly as the salt creeps in Case B than in Case A.

For $d_b = 3.0$ mm, the Case A and B results are not equivalent at higher porosities (Figure 4-3 and Figure 4-4). The reason for this is that humidity creep rate significantly decreases as backfill grain size increases. This means that, for $d_b = 3.0$ mm, the dislocation creep term is comparable in size to the humidity creep term for all porosities, meaning both terms always contribute to the overall creep.

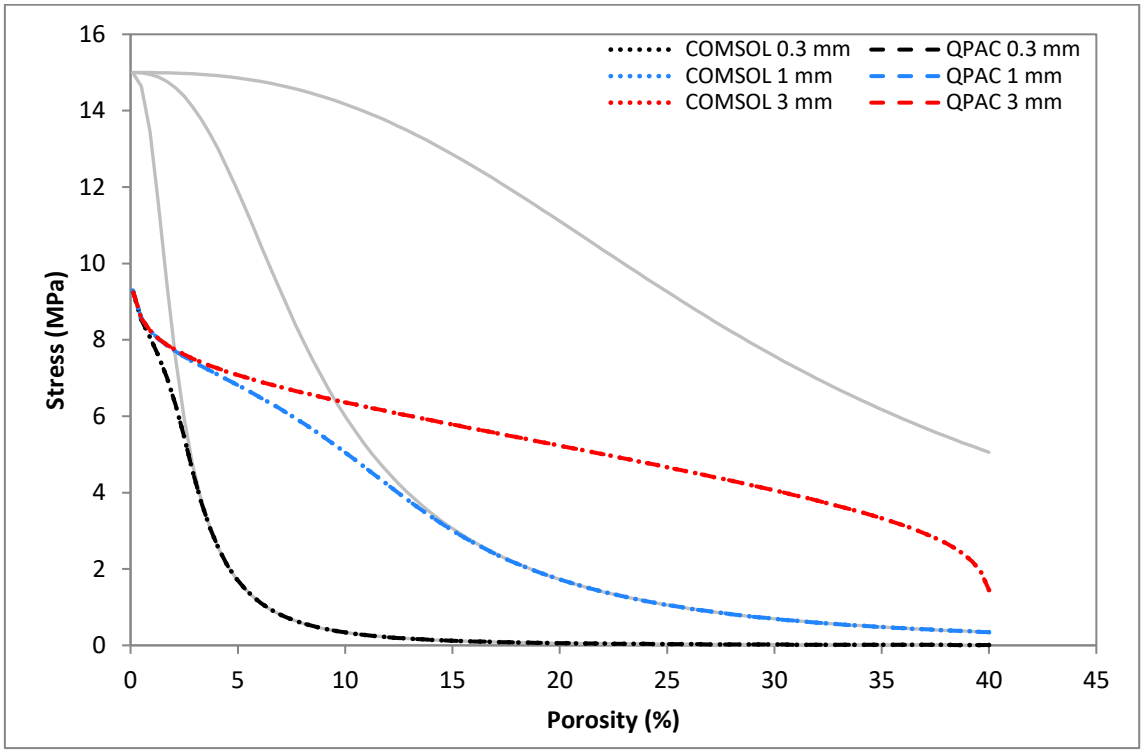

Figure 4-3: Mean Terzaghi effective stress against porosity for three backfill grain sizes (Case B). The case A results are shown in light grey, for reference.

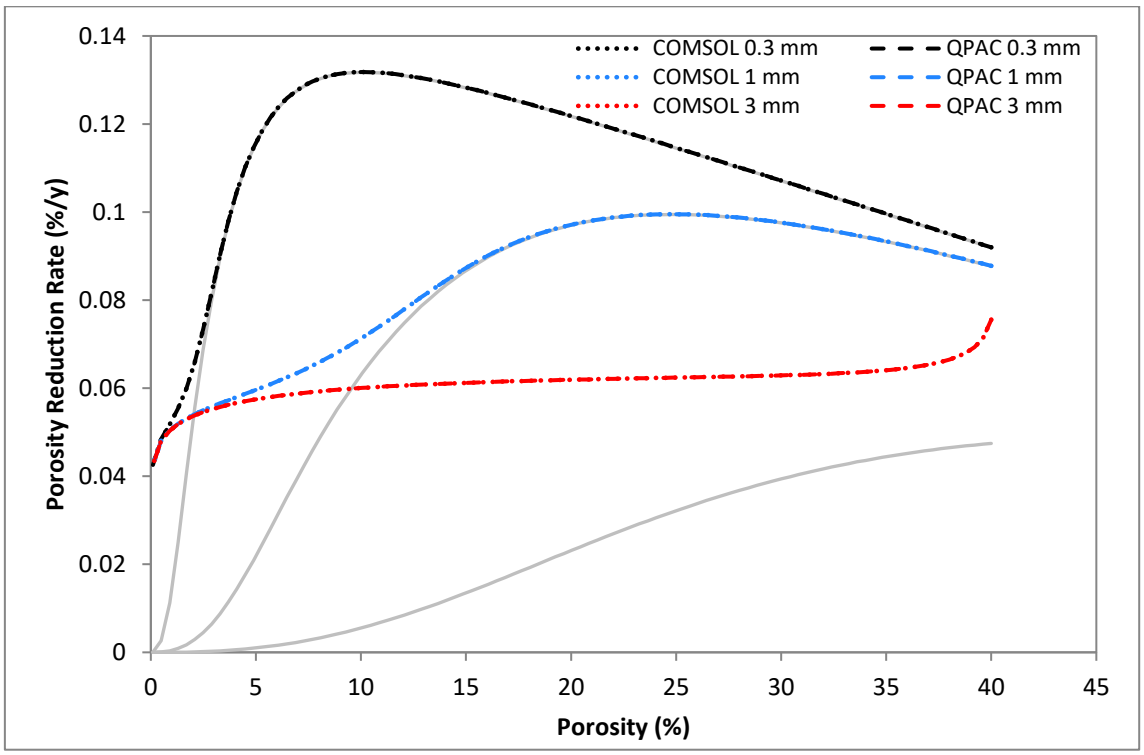

Figure 4-4: Porosity reduction rate against porosity for three backfill grain sizes (Case B). The case A results are shown in light grey, for reference.

4.3 Case C

Temperature in the repository is taken from Smit (2022, as reported in Benbow et al 2023) and is shown in Figure 4-5. The temperature profile consists of an initial sharp peak, followed by a gradual decay towards a final temperature of T ~ 37°C. For Case C, good consistency was again obtained between the COMSOL and QPAC implementations (Figure 4-6 and Figure 4-7). The impact of the temperature change can be most clearly assessed by plotting porosity as a function of time, as shown in Figure 4-8 for all three static cases and a fixed backfill grain size of $d_b = 3.0$ mm. The Case A and B results coincide until about $t \sim 350$ y, and then deviate due to the dislocation creep term, which cases the salt to creep faster in Case B than Case A, as discussed above. In Case C, however, the salt crept significantly faster than in both Case A and Case B. For both modes of creep in the backfill, creep rate is known to increase with temperature hence, given that the temperature function in Figure 4-5 exceeds 39.85°C for all result times considered, the faster creep in Case C was expected.

It was noted that there is a kink in the porosity results when the final porosity is reached (Figure 4-8). As described in section 3, the reason for this is that COMSOL immediately shuts down creep once the final porosity of 0.1% is reached, resulting in a discontinuity in the porosity reduction rate.

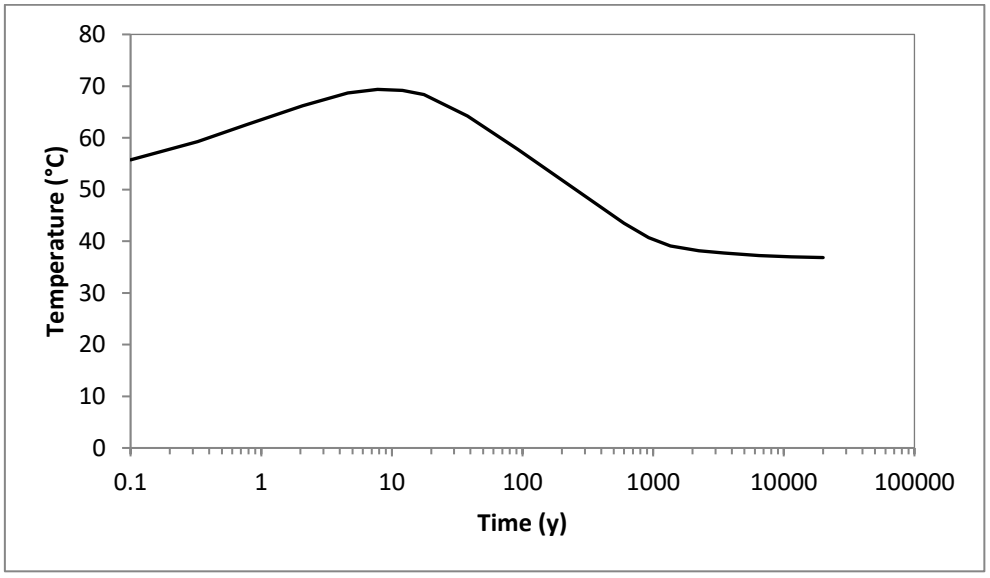

Figure 4-5: Illustrative temperature change used for static Case C (Benbow et al., 2023). For times outside the plotted range, temperature was assumed to be constant and equal to its earliest or latest value on the plot.

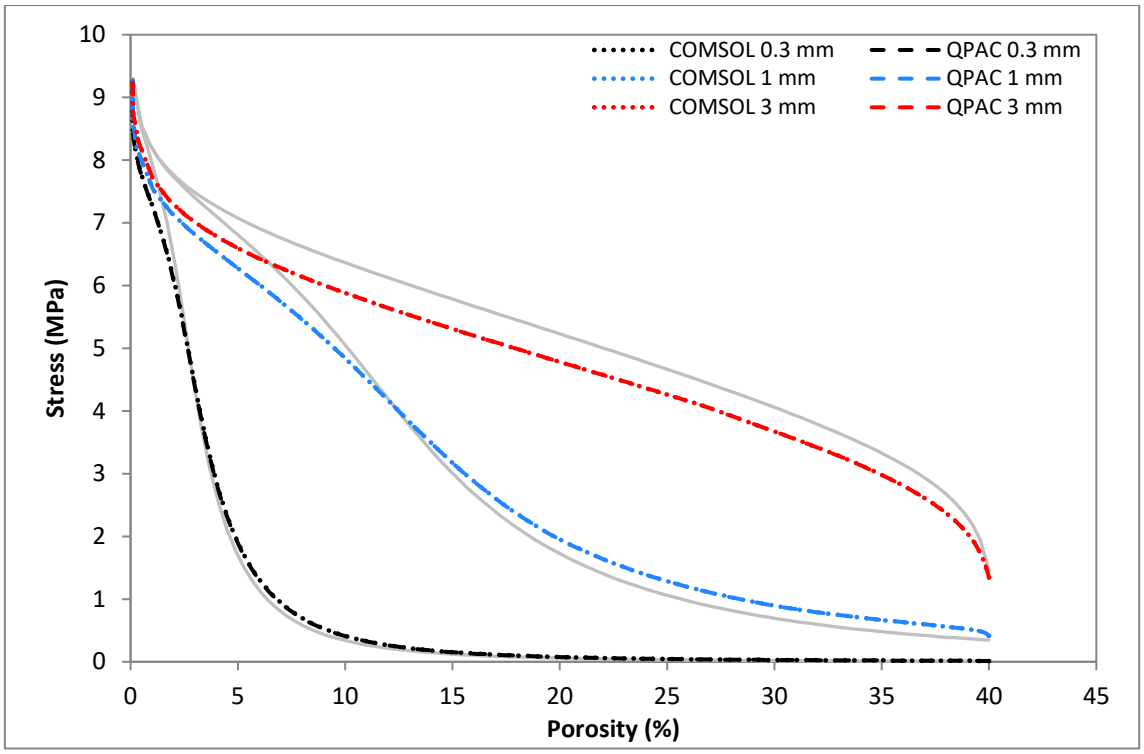

Figure 4-6: Mean Terzaghi effective stress against porosity for three backfill grain sizes (static Case C). The Case B results are shown in light grey, for reference.

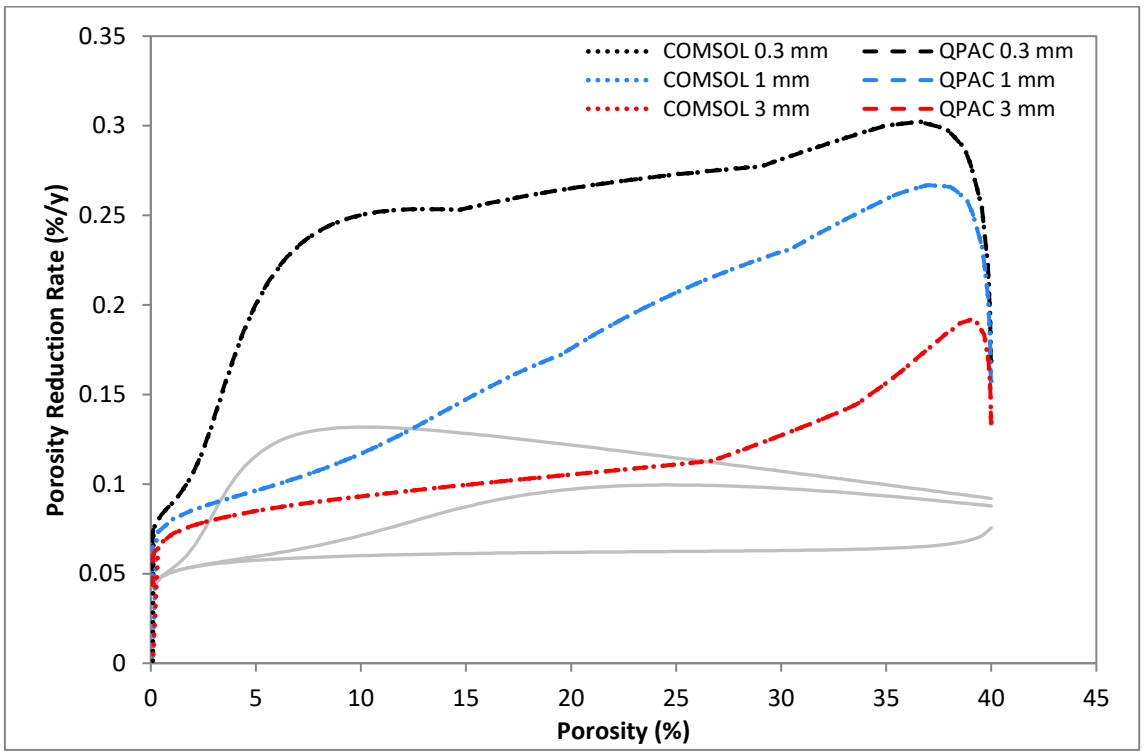

Figure 4-7: Porosity reduction rate against porosity for three backfill grain sizes (static Case C). The Case B results are shown in light grey, for reference.

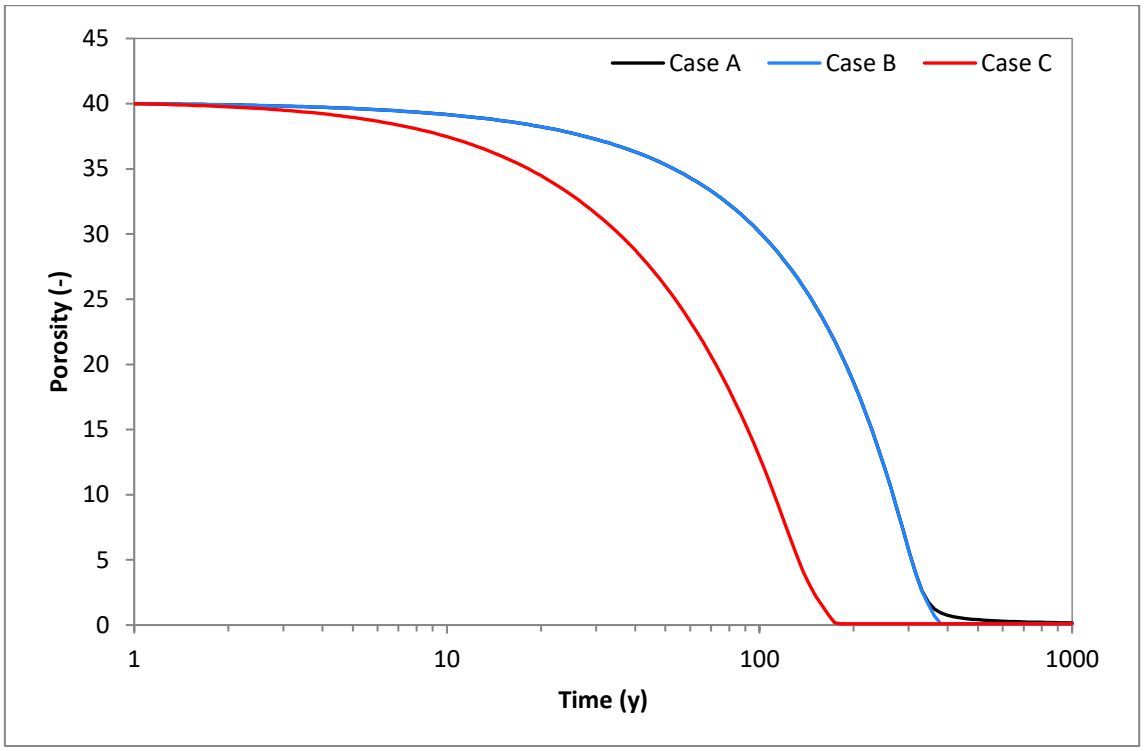

Figure 4-8: Porosity as a function of time for cases A, B and C ($d_b = 0.3$ mm).

5 Coupled Testing

To test the coupling of the creep model to a water flow model, we have implemented a simplified repository model, shown in Figure 5-1.

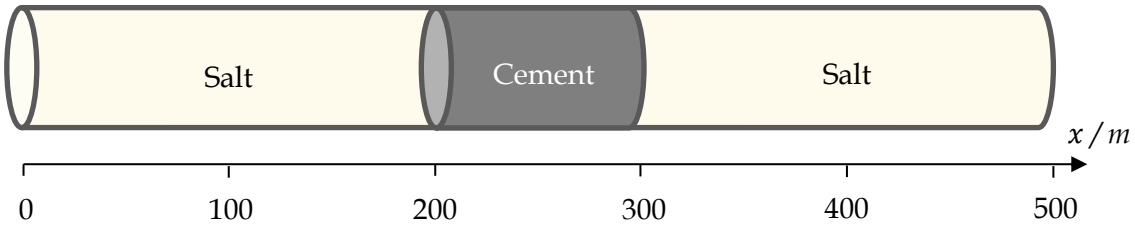

Figure 5-1: Simplified repository model. $x = 0$ m is a no flow boundary. $x = 500$ m is held at hydrostatic pressure.

The model consists of a 1D tunnel, 500 m in length. At the centre of the tunnel is a 100 m sorel cement plug, and the two 200 m regions on either side are backfilled with crushed salt, assumed to undergo mechanical creep of the form described in Section 2. The porosity of the crushed salt was calculated by the creep model (see below) and, as described in LaForce T et al. (2022), the permeability of the crushed salt was related to its porosity by

$$k = 1.89 \times 10^{-10}[m^2]\left(\frac{\phi}{100}\right)^{4.355} \quad \text{Eq. 4}$$

(A new parameter, `Crushed_Permeability_Model`, was defined to implement this equation). All other properties of the crushed salt and cement were taken directly from Bartol J (2023). To model groundwater flow in the tunnel, a Richards' Equation model was implemented, assuming a unit cross sectional area and reference pressure level of 1 atm. Richards' Equation was used to be consistent with COVRA's own modelling (Bartol, 2023), although only saturated flow is considered in this test model. Constant water density of $\rho = 10^3$ kg/m^3 and a dynamic viscosity of $\mu = 10^{-3}$ Pa·s were assumed, and for both materials, a van Genuchten-type retention model was adopted, with parameters as defined in Bartol (2023). At $x = 0$ m, a no flow boundary was assumed, and at $x = 500$ m, pore pressure was fixed at hydrostatic, assuming a repository depth of 850 m. The initial pore pressure across the entire domain was specified as hydrostatic, although COMSOL then calculated a steady state solution to use as its initial conditions.

The equations for water flow and creep are coupled by:

- Porosity, which is calculated by the creep equations in the salt. An additional mass term must be added to the Darcy flow equations, so pore pressure increases as porosity decreases. This term is given by $\frac{d}{dt}(\rho\phi S_e)$, where S_e is the effective saturation of the water in the salt.

- Stress. Eq.2 assumes that no pore pressure build-up during convergence, so effective stress which causes deformation of the salt backfill is equal to total stress which causes convergence of the host rock. To account for pore pressure build up, stress as calculated by Eq. 1 is the effective stress and the terms in Eq. 2 which refer to the host rock are updated so that stress is total stress (effective stress plus water pressure). The effective stress in terms 1 and 2 of Eq. 2, or `Strain_Rate_1` and `Strain_Rate_2`, were therefore replaced with the total stress, i.e.,
    - $\alpha_1 A_1 (P - \bar{\sigma})^{n_1}$ was replaced with $\alpha_1 A_1 \left(P - (P_w + \bar{\sigma})\right)^{n_1}$, and
    - $\alpha_2 A_2 (P - \bar{\sigma})^{n_2}$ was replaced with $\alpha_2 A_2 \left(P - (P_w + \bar{\sigma})\right)^{n_2}$,

  where P_w is the pressure term from the Richards' module. Note that, although the water pressure could in principle be negative, representing suction, any negative pressures were set to zero before coupling the results back into the creep model as these suction pressures are not expected to significantly impact the convergence of the tunnels. (In the COMSOL case, the Richards' pressure is named `p`, and the strictly positive version is named `P_w`, which is then coupled back into the creep model)

The setup described above was solved using an extremely fine mesh, assuming $T = 20$°C and $d_b = 0.5$ mm, and the results matched expectations. To maintain continuous water flux across both ends of the plug, a linear pressure gradient was observed across the cement region, with higher pore pressure on the no-flow side of the tunnel, and lower pore pressure on the hydrostatic side (Figure 5-2). Compaction in the backfill occurred significantly faster for the region of lower pore pressure than the region of higher pore pressure (Figure 5-3). This result makes sense, since high pore pressure will provide additional resistance against strain in the in-situ salt, reducing the effective stress on the backfill, and thus reducing its compaction rate. The system reaches an equilibrium pressure profile, with lithostatic conditions everywhere except the region around the hydrostatic boundary condition at $x = 500$ m.

The salt backfill did not compact everywhere. Instead, the porosity at which the backfill converged decreased as x increased (Figure 5-4). The reason for this is that permeability in the salt falls off very quickly with porosity (Eq. 4), which shuts down creep in the salt (decreasing permeability increases pore pressure, and as pore pressure approaches lithostatic, effective stress in the salt drops to zero, preventing any further compaction.) The open tunnel has a lower initial pore pressure and a higher compaction rate than the closed tunnel, hence the backfill here has a greater opportunity to compact prior to the lithostatic conditions being reached. However, the only point to fully compact and reach $\phi = \phi_f$ was $x = 500$ m, since the pore pressure here is fixed at hydrostatic, allowing the creep process to continue unhindered.

Whilst coupled testing has been successfully performed, the model was sometimes unstable. The reason for this is that Eq. 2, a complex, non-linear equation, in principle

has more than one solution. Occasionally, the COMSOL solver would switch to an unintended root, resulting in unphysical results, for example negative effective stress, resulting in an increase in the backfill porosity, i.e., $\dot{\phi} > 0$.

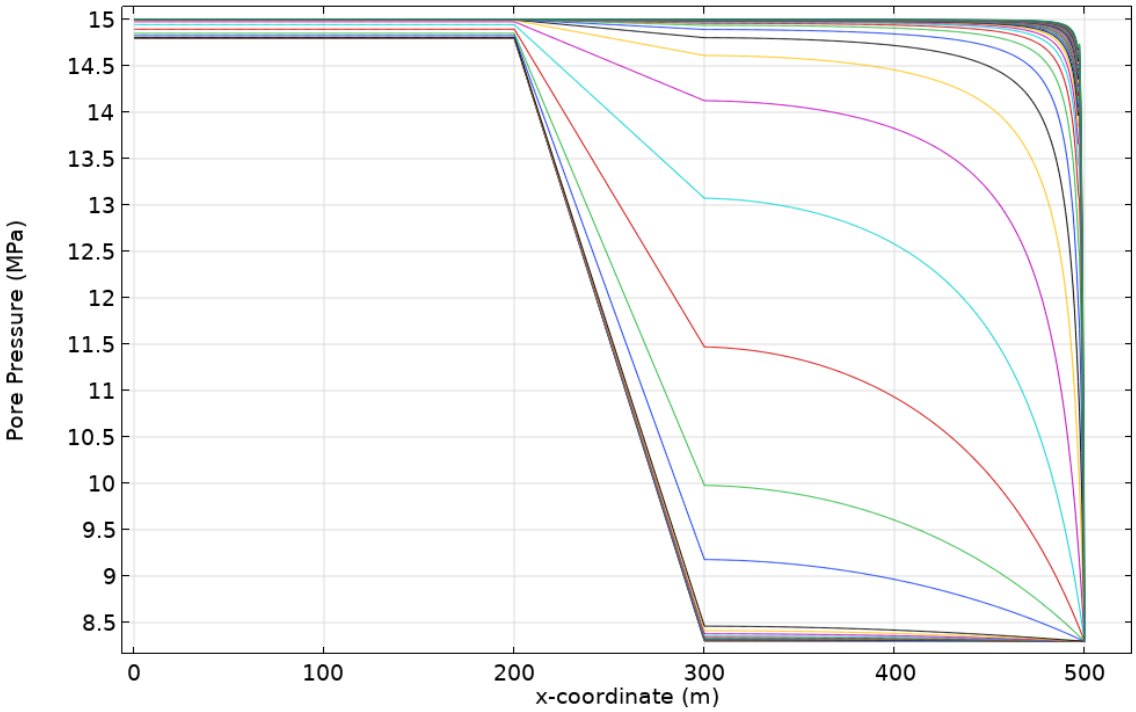

Figure 5-2: Pore pressure against x-coordinate, for $0 \leq t \leq 5000$ y.

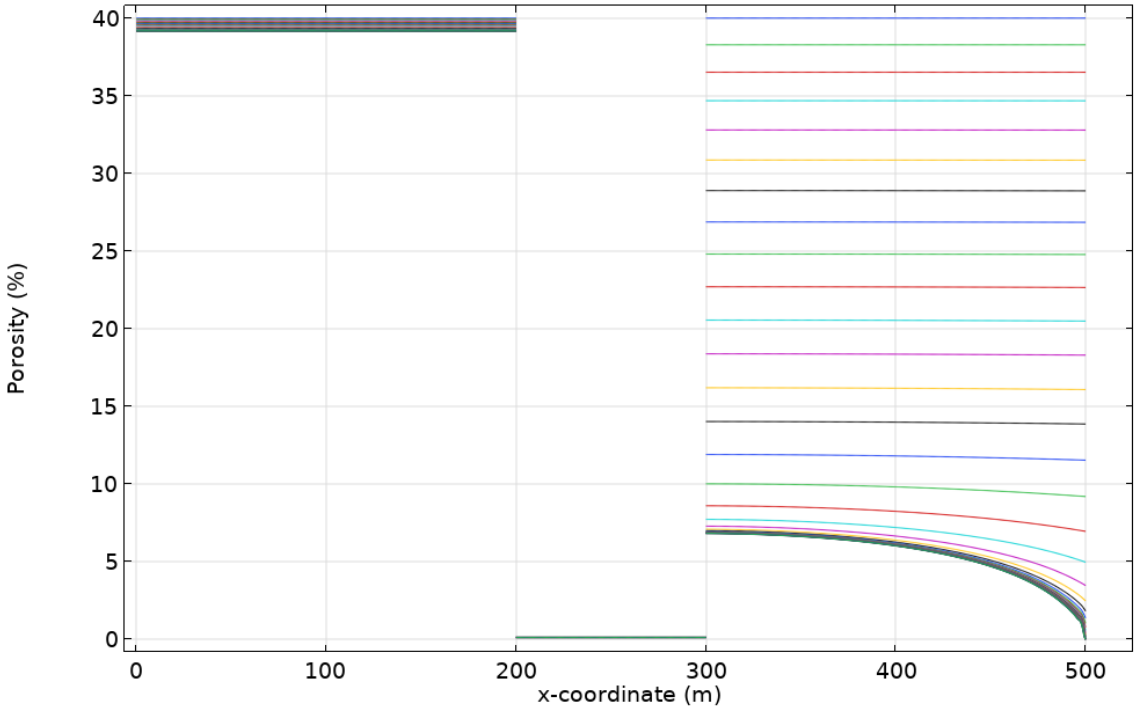

Figure 5-3: Porosity against x-coordinate, for $0 \leq t \leq 5000$ y.

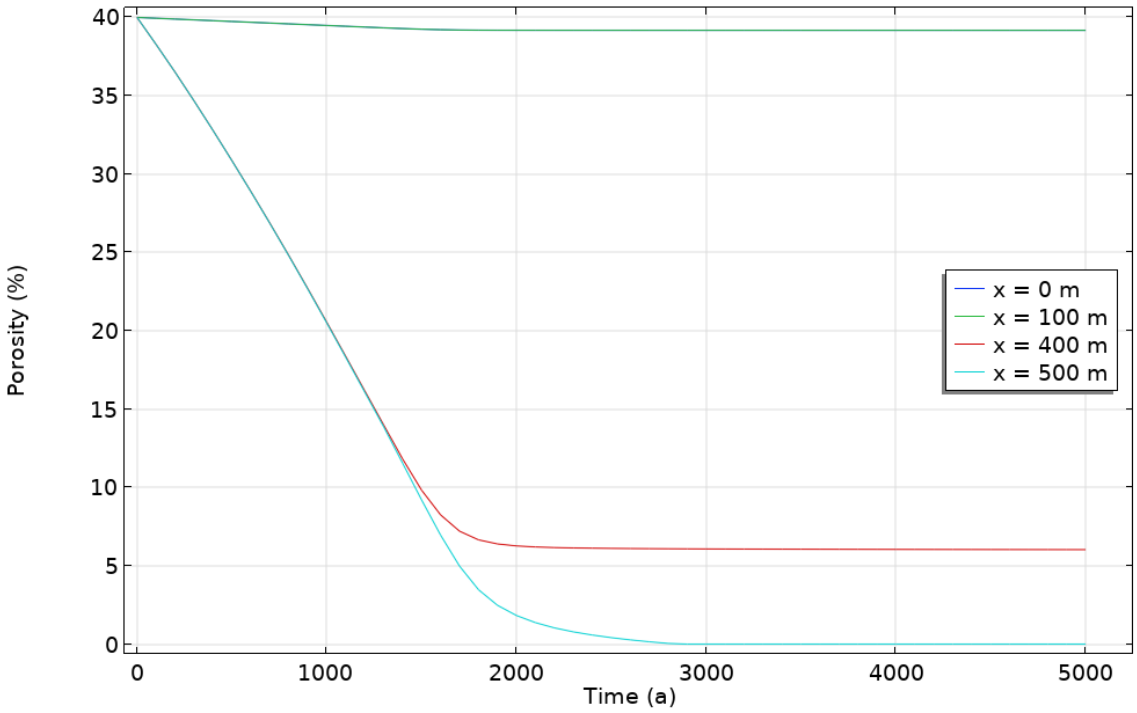

Figure 5-4: Porosity against time, reported at four locations in the domain ($x = 0$ m, $x = 100$ m, $x = 400$ m and $x = 500$ m.)

6 Conclusions / Summary / Further work

The numerical model described in van Oosterhout et al. (2022) has been successfully implemented in COMSOL Multiphysics®. The results in van Oosterhout et al. (2022b) have been successfully reproduced, and the model has been shown to produce physically-sensible results, both when employed on its own, and when coupled to Richards' Equation.

Future work might explore the behaviour of the model when implemented within a larger system, with additional processes or more complex geometry, for example, a generic model of a geological disposal facility in salt host rock. The behaviour of Eq. 2 might also be investigated in more detail, and in particular, methods to ensure that the solver consistently finds the intended root of this equation.

7 References

Bartol J (2023). COMSOL model provided to Quintessa.

Benbow S, Newson R, Bruffell L, Bond A and Watson S (2023). Potential Gas Generation in a Salt Repository. Gas generation model – Functional specification and definition of central case for analysis. Quintessa Report for COVRA. QDS-10075A-T2-FS Version 1

LaForce T, Jayne R, Leone R, Mariner P, Stein E and Nguyen S (2022). DECOVALEX-2023 Task F Specification Revision 9. Sandia National Laboratory report SAND2022-10439R.

Smit, H., 2022. *Long term disposal of nuclear waste in the Netherlands: possibilities and questions to be asked*. (COVRA)

van Oosterhout BGA, Hangx SJT, Spiers CJ and Bresser JHP (2022). Preliminary recommendations for modelling compaction creep and porosity-permeability evolution in crushed salt backfill: Phase 1 Deliverable. Report to COVRA from Utrecht University.

van Oosterhout BGA, Hangx SJT, Spiers CJ and Bresser JHP (2022). Recommendations for modelling evolution of a backfilled repository: Deliverable I - Discussion. Powerpoint presentation by Universiteit Utrecht to COVRA.

Watson S (2023). Gas Generation in a Salt Repository Waste Groups and High-level Conceptualisation. Quintessa report for COVRA. QDS-10075A-T1-WASTES Version 1.1